Generation of picosecond pulses directly from a 100 W, burst-mode, doping-managed Yb-doped fiber amplifier

P. Elahi,[1],* S. Yılmaz,[1] Y. B. Eldeniz,[2] and F. Ö. Ilday[1]

[1]*Department of Physics, Bilkent University, 06800 Ankara, Turkey*
[2]*Department of Electrical and Electronics Engineering, Ankara University, 06100 Ankara, Turkey*
*Corresponding author: pelahi@fen.bilkent.edu.tr

Burst-mode laser systems offer increased effectiveness in material processing while requiring lower individual pulse energies. Fiber amplifiers operating in this regime generate low powers in the order of 1 W. We present a Yb-doped fiber amplifier, utilizing doping management, that scales the average power up to 100 W. The laser system produces bursts at 1 MHz, where each burst comprises 10 pulses with 10 µJ energy per pulse and is separated in time by 10 ns. The high-burst repetition rate allows substantial simplification of the setup over previous demonstrations of burst-mode operation in fiber lasers. The total energy in each burst is 100 µJ and the average power achieved within the burst is 1 kW. The pulse evolution in the final stage of amplification is initiated as self-similar ampli-fication, which is quickly altered as the pulse spectrum exceeds the gain bandwidth. By prechirping the pulses launched into the amplifier, 17 ps long pulses are generated without using external pulse compression. The peak power of the pulses is ~0.6 MW.   © 2014 Optical Society of America

OCIS codes: (060.3510) Lasers, fiber; (140.3280) Laser amplifiers; (140.3615) Lasers, ytterbium; (140.7090) Ultrafast lasers.
http://dx.doi.org/10.1364/OL.39.000236

Among the diverse applications of ultrafast lasers, material processing has long been predicted to develop into a major application area [1,2]. At the present time, industrial material processing in this regime continues to be dominated by solid-state gain media due to the rel-atively low pulse energies that are generated from fiber lasers. While there are increasingly many reports on rod-type fiber lasers covering the range from several 10 µJ to 1 mJ in pulse energy [3], these systems offer this performance at a cost of increased complexity in the ex-perimental setup. There is clearly demand for simple, highly integrated fiber systems based on off-the-shelf fiber-optical components, offering ~10 µJ energies and picosecond pulse durations.

A particularly interesting mode of laser operation is the so-called burst mode operation, wherein the amplifier in-termittently produces pulses at very high repetition rates. Some applications of burst mode include photoacoustic microscopy [4], laser ablation of materials [5], and photo-injector drive lasers at accelerator facilities [6]. Burst mode offers major advantages in material processing, since each burst has a material-ablation effect similar to that of a single pulse of energy equal to that of the en-tire burst, as long as the instantaneous repetition rate within the burst is above a threshold determined by the thermal conductivity of the material [7]. Recently, we have shown, for the first time, burst-mode operation of a highly integrated fiber amplifier, offering 20 µJ pulses with 0.25 mJ energy within one burst [8]. This was fol-lowed by [9], which broke the 1 mJ energy per barrier, with individual pulse energies of 40 µJ. The expected in-crease in ablation rate has been confirmed with this sys-tem [10]. Both of these systems were built using off-the-shelf components and step-index fibers, operated at 1 kHz, corresponding to a modest average power of 1 W. Using rod-type fibers, Breitkopf *et al.*, have obtained 58 mJ burst energy at 20 Hz repetition frequency with the average power of ~1.6 W [11]. While these systems represent advancements of the state of the art, practical material processing demands much higher average powers, of which fiber lasers are capable.

Average and peak power levels are generally limited by thermal and nonlinear effects, respectively, and obtaining high average and peak pulses simultaneously requires competing solutions. In order to partially miti-gate this trade-off, we have recently proposed doping management, which utilizes fibers with continuously or discretely changing doping levels along the gain fiber, generating 4.5 ps pulses at 100 W and 100 MHz [12]. Other recent reports on high-power fiber amplifiers with regu-lar fibers include 110 W, subpicosecond pulses at 1.3 GHz [13] and 125 W, 13 ps pulses at 1 GHz [14].

Here, we report burst-mode operation of a Yb-doped fiber laser at 100 W of average power with 10 µJ individ-ual pulse and 100 µJ burst energy. These results scale the burst-mode operation of fiber amplifiers from the ~1 W level to 100 W level for the first time. From a material processing point of view, it is highly desirable to achieve pulse energy of 10 µJ and burst energy of 100 µJ, while keeping the pulse duration 15–20 ps to reap the benefits of ultrafast ablation [7]. We designed the system to gen-erate sub-20 ps pulses directly to avoid the use of exter-nal compression, which is costly and challenging at 100 W. To this end, we employ negative prechirping of the pulses as they traverse through the final amplifier, initially undergoing self-similar amplification [15,16], compensating for part of the nonlinear effects, before spectral broadening due to Raman scattering begins to dominate. We implement discrete doping management in the final power amplifier to manage the thermal load while keeping fiber length relatively short to minimize the nonlinear effects to achieve the shortest pulse duration [12].

The schematic of the experimental setup is shown in Fig. 1. The oscillator is a home-built passively mode locked all-normal-dispersion (ANDi) laser with a
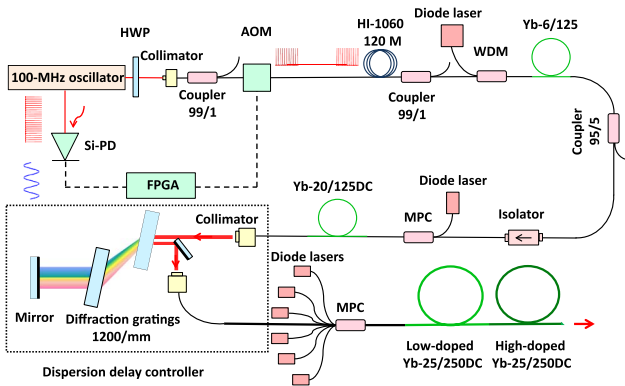
Fig. 1.   Schematic of the setup. FPGA, field-programmable gate array; AOM, acousto-optic modulator; WDM, wavelength-division multiplexer; MPC, multipump combiner; Si-PD, silicon photodetector.

repetition frequency of 100 MHz, generating 3.6 ps long chirped pulses with a spectral bandwidth of 9 nm. We use the 80 mW output from the polarization rejection port to seed the amplifier. After coupling the beam into a fiber collimator, the pulse train is modulated by a fiber-integrated acousto-optic modulator (AOM) with insertion loss of 3 dB and 10 ns rise time, picking up 10 pulses of the oscillator every 1 µs, carving out 10 pulse bursts with a repetition rate of 1 MHz. A field-programmable gate-array (FPGA) device is employed to drive the AOM. The FPGA is triggered by the optical signal obtained from the oscillator after converting to an electrical signal in an amplified silicon photodetector. Thanks to the high repetition rate of 1 MHz for the bursts, amplified spontaneous emission between the bursts is negligible, which is why pulsed pumping of the amplifier stages is not necessary [8]. In addition, variation of the effective gain as experienced by the pulses at the beginning and end of the burst is relatively small. For this reason, we do not need to preshape the individual pulse energies within the burst in order to equate their energies at the end of the amplifier chain [9]. Thus, the high average powers, which make it possible to operate at MHz-level repetition rates with microjoule energies, simplifies the electronics and the pumping scheme substantially over previous demonstrations of burst-mode operation of fiber amplifiers.

Following the AOM, the average power is reduced to 0.84 mW. The pulses are first stretched to 51 ps in a 120 m long HI 1060 fiber and then amplified up to 117 mW in the first stage of the amplifier chain, which is made of 80 cm of highly doped Yb-doped gain fiber (Yb 501, CorActive) with 500 dB/m absorption at 976 nm. The core diameter of the single-clad, core-pumped fiber is 6 µm. The spectral and temporal widths after the first stage amplifier are ∼13 nm and 49 ps, respectively. The slight reduction in width is due to gain filtering. This is followed by the second-stage amplifier, composed of a 140 cm long Yb-doped double-clad fiber with 20 µm core diameter and 125 µm inner cladding diameter. The cladding absorption of gain fiber is 2.3 dB/m at 976 nm. A $(2 + 1) \times 1$ pump combiner was employed to deliver pump light from a multimode diode laser coupled to a 105 µm fiber to the cladding region of the gain fiber. The maximum power of the diode is 25 W. This allows us to scale up

the average output power of the second amplifier to 6.5 W at a pump power of 12 W. The power is kept at this level to avoid damage to the optical gratings that follow. Because of additional gain filtering, the spectral width is measured to be 11 nm. The pulse duration is ∼41 ps and the pulse energy is ∼650 nJ. The nonlinear phase shift accumulated in this stage is kept small, around 4π, as a result of the stretching of the pulses and by keeping the lead of the collimator to 100 cm.

In order to control the chirp of the pulses launched into the final amplifier stage, a dispersive delay line (DDL) based on transmission type diffraction gratings with groove density of 1200 line/mm is placed after the second stage amplifier. Group velocity dispersion of the DDL is calculated to be −11400 fs²/mm. The distance between the gratings is adjusted precisely with a translation stage and the chirp of the pulse is, in turn, set to minimize the pulse duration, which is measured after the final power amplifier. The total length of the fibers in this system is 134 m and together with dispersion of −2.56 ps² from the DDL, the total group dispersion delay is adjusted to a calculated value of 0.16 ps² to achieve the shortest output pulse duration at full power. The corresponding pulse duration after the DDL is calculated to be around 7 ps (positively chirped).

A high-power-compatible fiber-pigtailed collimator allows easy coupling of the beam after the DDL to the power amplifier. The power amplifier implements doping-management, composed of two gain fiber segments with different doping concentration level, similar to that in [12]. A $(6 + 1) \times 1$ pump-signal combiner is used to deliver pump light from six 25 W fiber-pigtailed diode lasers to the gain segments. The first gain segment is a 1.8 m long low-doped double-clad Yb fiber with 25 µm core diameter and 250 µm inner cladding diameter with 2.5 dB/m cladding absorption at 976 nm and the second segment is a 1.6 m long high-doped Yb fiber with an identical geometry, but with 3.5 dB/m cladding absorption at 976 nm. The identical geometry of the gain fibers means that their splicing is absolutely the same as splicing two pieces of the same fiber or splicing to the lead fiber of the pump-signal combiner. The length of each segment is optimized to achieve a good trade-off between nonlinear phase accumulation and thermal load. The output of the gain fiber is also angle-cleaved to prevent back reflected light from getting coupled back into the core and to avoid its amplification, lest it can cause system damage. Since pump diodes are not wavelength-stabilized, their central wavelength shifts as a function of their operating current and temperature, which in turn affects the absorption in the gain segments. In order not to deviate from the optimization of doping management, the central wavelengths of the diodes are stabilized using a feedback system to set the temperature of the diodes and ensure the output wavelength remains at 976 nm at all times. The total pump power of the amplifier is 150 W and boosts the 1 W input seed up to 100 W. At the present time, the output power is limited by the available pump power and based on our experience with the same fiber types and pump combiner without a signal port, but with a larger number of ports for CW operation, at least 200 W should be possible to support using the same fibers and with the present doping-management scheme.

Almost all of the nonlinear pulse shaping of the entire system takes place in the last 2 m of the final stage of amplification, the power amplifier. The launched pulse energy and duration are 100 nJ and 6 ps, respectively. The conditions initially are supportive of self-similar amplification [15], but the evolution deviates from self-similar evolution early on since the spectrum broadens beyond the gain bandwidth [16]. As the pulse energy is increased, nonlinear effects get stronger, resulting in rapid spectral broadening. Intrapulse Raman scattering becomes significant, transferring energy to longer wavelengths, together with the influence of self-phase modulation (SPM) and four-wave mixing, resulting in highly asymmetrical spectral broadening. The estimated nonlinear phase shift is approximately 130π, although it must be emphasized that nonlinear phase shift is not a good metric to characterize the strength of nonlinear effects, given the extreme spectral reshaping and that the dominant role shifts from SPM to Raman scattering after a brief period of SPM-dominated evolution. SPM and gain filtering continue to act on the portion around 1060 nm, but the Raman effect continuously and effectively pumps energy to the longer wavelengths. Figure 2 shows measured optical spectra in linear (a) and logarithmic (b) scales for 20, 60, and 100 W output power, corresponding to 2, 6, and 10 μJ individual pulse energies, respectively. The corresponding spectral widths (measured at –3 dB) are 110, 200, and 240 nm, respectively. At the highest power of 100 W, the spectrum resembles that of supercontinuum generation, achieving a width of 320 nm, if measured at the –10 dB points. The underlying dynamics are complex, containing elements of coherent supercontinuum generation with femtosecond pulses, as well as those of incoherent supercontinuum generation with nanosecond pulses [17]. These complex dynamics represent new opportunities for control of nonlinear effects, the details of which will be analyzed in a separate publication.

The measured autocorrelation signals are presented in Fig. 3(a). The pulse widths are inferred to be 7, 14, and 17 ps at 20, 60, and 100 W output powers, respectively. We have used the PICASO algorithm based on the measured autocorrelation and spectrum to retrieve the pulse and the case of the full output power with a calculated pulse width of 17 ps is shown in Fig. 3(b). The variation of output spectral and pulse width of power amplifier versus output power is in Fig. 4(a). As can be seen here, the spectral and pulse widths increase with output power, showing that the nonlinear pulse shaping is deep into the spectral broadening regime that follows the brief

Fig. 3.   (a) Measured intensity autocorrelation burst mode operation at output powers of 20 W (dotted line), 60 W (dashed line), and 100 W (solid line). (b) Intensity autocorrelation measured at 100 W of output power (solid line) along with retrieved autocorrelation using PICASO (dashed line). Inset: retrieved pulse shape with FWHM of 17 ps.

episode of self-similar amplification for the chosen values of prechirping. The pulse burst generated from the power amplifier is shown in Fig. 4(b). The average energy of one burst is 100 μJ and the average energy for the pulses within the burst is 10 μJ. The largest (smallest) pulse energy in the burst is ~13 μJ (~7 μJ). The standard deviation is calculated to be 17%.

In conclusion, we have demonstrated a 100 W, picosecond Yb-doped fiber laser operating in the burst mode. The maximum average and peak powers are 100 W and 0.6 MW, respectively. The system generates ~10 μJ, 17 ps long pulses directly from fiber. Direct fiber delivery eliminates need for external pulse compression, which is difficult to obtain reliably and requires expensive bulk optics at this power level. Extremely strong nonlinear spectral shaping takes place in the last portion of the power amplifier, combining SPM, four-wave mixing, and intrapulse Raman scattering, resulting in the broadening the spectral width to 240 nm (320 nm), measured at the –3 dB (–10 dB) points. However, the spectral width is largely irrelevant for most material processing applications and the pulse duration remains short enough to exploit much of the benefits of ultrafast processing, particularly for metals. The repetition rate is high enough to simplify the pumping scheme and the associated electronics. Utilization of doping management results in a small penalty of 24% increase in the accumulated nonlinearity phase shift, as opposed to using only highly doped fiber, while reducing the thermal load by a factor of 2. We expect this system to find numerous applications in material processing, as well as niche applications, such as photoinjector lasers at accelerators.
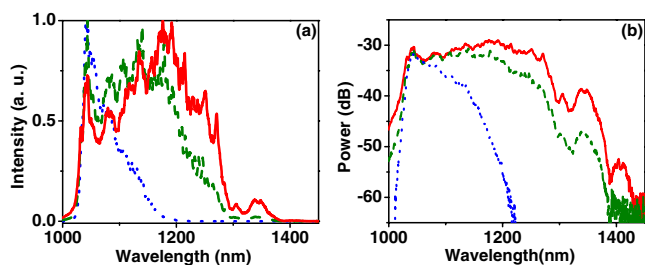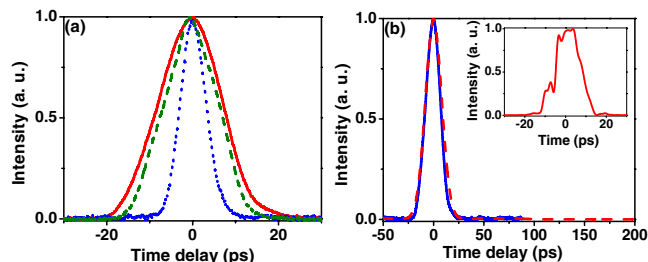

Fig. 2.   Measured optical spectra in burst mode operation at output powers of 20 W (dotted line), 60 W (dashed line), and 100 W (solid line), shown as (a) linear and (b) semi-log plots.
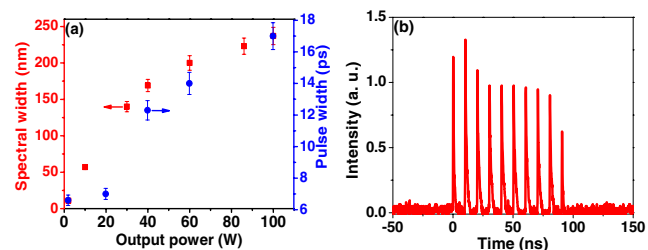

Fig. 4.   (a) Spectra width (squares) and pulse width (circles) versus output power. (b) Pulse train in one burst from power amplifier at 100 W output power. The pulse energy variation is 17%.

References

1. E. G. Gamaly, Phys. Rep. **508**, 91 (2011).
2. E. G. Gamaly, A. V. Rode, B. Luther-Davies, and V. T. Tikhonchuk, Phys. Plasmas **9**, 949 (2002).
3. F. Röser, T. Eidam, J. Rothhardt, O. Schmidt, D. N. Schimpf, J. Limpert, and A. Tünnermann, Opt. Lett. **32**, 3495 (2007).
4. T. Liu, J. Wang, G. I. Petrov, V. V. Yakovlev, and H. F. Zhang, Med. Phys. **37**, 1518 (2010).
5. M. Lapczyna, K. P. Chen, P. R. Herman, H. W. Tan, and R. S. Marjoribanks, Appl. Phys. A **69** [Suppl.], S883 (1999).
6. I. Will, H. I. Templin, S. Schreiber, and S. Sandner, Opt. Express **19**, 23770 (2011).
7. W. Hu, Y. C. Shin, and G. King, Appl. Phys. A **98**, 407 (2010).
8. H. Kalaycioğlu, K. Eken, and F. Ö. Ilday, Opt. Lett. **36**, 3383 (2011).
9. H. Kalaycioğlu, Y. B. Eldeniz, Ö. Akçaalan, S. Yavaş, K. Gürel, M. Efe, and F. Ö. Ilday, Opt. Lett. **37**, 2586 (2012).
10. C. Kerse, H. Kalaycioğlu, Ö. Akcaalan, B. Eldeniz, F. Ö. Ilday, H. Hoogland, and R. Holzwarth, in *CLEO Europe*, OSA Technical Digest (CD) (Optical Society of America, 2013), paper CM-P.26S.
11. S. Breitkopf, A. Klenke, T. Gottschall, H.-J. Otto, C. Jauregui, J. Limpert, and A. Tünnermann, Opt. Lett. **37**, 5169 (2012).
12. P. Elahi, S. Yılmaz, Ö. Akçaalan, H. Kalaycioğlu, B. Öktem, Ç. Şenel, F. Ö. Ilday, and K. Eken, Opt. Lett. **37**, 3042 (2012).
13. Z. Zhao, B. M. Dunham, I. Bazarov, and F. W. Wise, Opt. Express **20**, 4850 (2012).
14. H. W. Chen, Y. Lei, S. P. Chen, J. Hou, and Q. S. Lu, Appl. Phys. B **109**, 233 (2012).
15. M. E. Fermann, V. I. Kruglov, B. C. Thomsen, J. M. Dudley, and J. D. Harvey, Phys. Rev. Lett. **84**, 6010 (2000).
16. D. B. Soh, J. Nilsson, and A. B. Grudinin, J. Opt. Soc. Am. B **23**, 10 (2006).
17. J. M. Dudley and S. Coen, Rev. Mod. Phys. **78**, 1135 (2006).